Effect of the polypropylene type on polymer–diluent phase diagrams and membrane structure in membranes formed via the TIPS process Part I. Metallocene and Ziegler–Natta polypropylenes

Wilfredo Yave [a,*], Raúl Quijada [a], Daniel Serafini [b], Douglas R. Lloyd [c]

[a] *Departamento de Ingeniería Química, Facultad de Ciencias Físicas y Matemáticas, Universidad de Chile, y Centro para la Investigación Interdisciplinaria Avanzada en Ciencia de los Materiales (CIMAT), Casilla 2777, Santiago, Chile*
[b] *Departamento de Física, Universidad de Santiago, Santiago, Chile*
[c] *Department of Chemical Engineering, The University of Texas at Austin, Austin, TX 78712-1062, USA*

Abstract

Isotactic polypropylene (iPP) samples produced via Ziegler–Natta catalysts (iPPZN) and metallocene catalysts (iPPM) were used to investigate the effects of molecular weight and molecular weight distribution on the phase diagram for iPP–diphenyl ether systems and the morphology of membranes made from these systems. It was found experimentally that the molecular weight and molecular weight distribution influenced the location of the cloud point curve and the morphology of membranes produced via thermally induced phase separation. The influence on the cloud point curve was attributed to entropic and enthalpic considerations. The influence on membrane morphology was attributed to differences in the growth period (resulting from a shift in the cloud point and dynamic crystallization curves) and differences in system viscosity. All of these factors are related to the type of catalyst used to produce the iPP.

Keywords: Polypropylene–diphenylether phase diagram; Polypropylene; TIPS process

1. Introduction

Polypropylene has a wide variety of commercial uses as a commodity polymer [1–3]. One such use includes polypropylene membranes for applications that require good mechanical properties, thermal stability, and chemical resistance [4–7].

Using commercial isotactic polypropylene (iPP), many studies have been carried out on membrane preparation by the thermally induced phase separation (TIPS) process. This process was invented by Castro [8]. Wagener and co-workers [9] reported about the influences of type of polymer, polymer concentration, cooling rate, type and molecular weight of diluent on pore structure. Later, Lloyd et al. [10–12] investigated the effect of the system's thermodynamic interactions, cooling conditions, phase separation mechanism, etc. on membrane structure. Matsuyama et al. [13] studied the effect of the polypropylene molecular weight on membrane structure, and showed that the binodal curve shifts to lower temperatures as the polymer molecular weight is decreased. They also investigated the kinetics of the TIPS process [14]. Lee et al. [15] also showed that the binodal curve decreases with decreasing polypropylene molecular weight. McGuire et al. [16] studied the coarsening process for droplets formed by the phase separation, simulated the coarsening process, and showed that the coarsening rate theoretically obtained agreed well with the experimental data.

As outlined above, polypropylene membrane preparation has been studied extensively to understand the phase separation behavior in the TIPS process and how that relates to membrane morphology. However, in all the studies traditional

* Corresponding author. Tel.: +56 2 6784188; fax: +56 2 6991084.
E-mail address: wyave@ing.uchile.cl (W. Yave).

commercial polypropylenes prepared using Ziegler–Natta catalysts have been used. Research has found that these catalyst systems can be used to produce polymers that differ in both tacticity and molecular weight. The discovery and development of metallocenes catalysts initiated an enormous interest in the polymerization of olefins and their application [17–22]. These catalysts are capable of producing polymers with a well-defined microstructure, such as isotactic, syndiotactic, stereoblock, etc., with similar molecular weight and defect distribution [23–28]. Therefore, the difference between commercial polypropylene obtained with a Ziegler–Natta catalyst and with a metallocene is the molecular weight distribution and crystalline morphology [29–31].

On the other hand, iPP is a polymer with unique morphological properties, and the relationship of configurational chemistry, chemical species, and physical states interact to determine the stable phases and thermodynamic properties. Little has appeared in the open literature describing the properties of iPP prepared with metallocene catalysts.

It is well known that in membrane preparation by the TIPS process, the thermodynamic properties of the polymer–diluent system can affect the final morphology [8–13,32]. Phase diagrams provide much information on phase behavior of the polymer–diluent system, and they are important to understand the resulting morphology of the membranes. Molecular weight and molecular weight distribution can have significant impact on the location and shape of the phase diagram and therefore on the final membrane morphology. These effects have not previously been studied, and membrane preparation from iPP obtained by metallocene catalysts has not been reported.

The present work was intended to show how the catalyst type affects the phase diagram and membrane morphology through molecular weight and molecular weight distribution. Commercial polymers obtained via Ziegler–Natta catalysts (iPPZN) were used, as well as polymers produced in our laboratories with metallocene catalyst (iPPM). Phase diagrams were obtained for six polymer–diluent systems in order to study the effect of molecular weight distribution on the location of the binodal and melting point depression curve. Membranes were prepared from the two polymer–diluent systems and the final morphologies were compared using scanning electron microscopy (SEM). In addition, droplet growth kinetics was monitored for the polymer–diluent systems to determine the effects of molecular weight distribution on the kinetics of structure development.

2. Materials and methods

2.1. Materials

A total of six polypropylene samples were used in this work. Three were commercial iPPZN and three were iPPM prepared in our laboratory with metallocene catalysts [33]. The molecular weight properties ($\bar{M}_w$ and $\bar{M}_w/\bar{M}_n$) determined by gel permeation chromatography (GPC) and the thermal properties (T_m and ΔH_f) obtained by differential scanning calorimetry (DSC) are given in Table 1.

Diphenylether (DPE) from Aldrich was used without further purification as diluent for membrane preparation. Methanol (Aldrich) was used to extract the DPE from the polymer matrix.

2.2. Methods

2.2.1. Phase diagrams

To obtain the phase diagrams, solid polymer–diluent samples with different concentrations were prepared as outlined in the next section of this paper. A portion of the solid sample was loaded into capillary tubes; the capillary tube was purged with nitrogen, sealed to prevent oxidation, and heated in a 9100 (Merck) electrothermal equipment at 453 K. After waiting for at least 5 min to ensure complete melting, the samples were cooled at 10 K/min. The cloud point was determined visually by noting the first appearance of turbidity under optical eyeglasses incorporated in the electrothermal equipment. The values obtained are presented as the arithmetic mean of the three measurements; the error was less than 2 K.

Dynamic crystallization temperatures were determined calorimetrically using a Modulated TA Instruments DSC290 Differential Scanning Calorimeter (DSC). In this case the samples were prepared in the same way as above, but the cooling was done suddenly in liquid nitrogen to ensure a homogeneous solid solution. Then, a small portion of the solid solution was cut and used for the thermal analysis at a cooling rate of 10 K/min.

2.2.2. Membrane preparation and SEM analysis

The TIPS process was used to prepare the membranes. This method has been described by Lloyd et al. [5,10]. Polymer–diluent samples (20 wt.% polymer) with an antioxidant (IRGANOX1010/IRGAFOS168, 0.02 wt.%) were pre-

Table 1
Basic properties of the isotactic polypropylenes

Materials	$\bar{M}_w$ (kg/mol)	$\bar{M}_w/\bar{M}_n$ (K)	T_m	ΔH_f (J/g)	Crystallinity (%)
iPPZN-340 (FINA)	340	4.0	439	85.6	41.1
iPPZN-260 (Petroquim)	260	4.5	438	85.7	41.0
iPPZN-160 (Petroquim)	160	4.4	443	94.9	45.4
iPPM-340 (U-Chile)	340	1.8	425	85.8	41.0
iPPM-260 (U-Chile)	260	1.9	424	90.9	43.5
iPPM-160 (U-Chile)	160	1.8	423	93.0	44.5

pared in a test tube that was purged with nitrogen and sealed to prevent oxidation. The test tube was placed in an oven at 453 K for 48 h to homogenize the solution, and was then immersed in liquid nitrogen in order to induce solidification. A small portion of the solid solution was taken and placed on a circular thin film of aluminum (thin film sample of 500 μm and 5 cm of diameter) and covered with Teflon. This assembly was heated in an oven at 453 K for 5 min, and it was then cooled immediately by immersion in ice water. Loss of DPE during this stage was experimentally determined to be less than 3 wt.%. Finally, DPE in the membrane was extracted with methanol, and the methanol was evaporated to produce microporous membranes.

Membrane structures were examined by TESLA BS343A Scanning Electron Microscopy (SEM) at an accelerating voltage of 15 kV. The samples were fractured in liquid nitrogen, and a small piece was coated with gold in vacuum to examine the membrane cross-section.

2.2.3. Droplet growth process

The droplet growth process was studied using a hot stage (Mettler FP82HT), which was placed on the platform of an optical microscope (Nikon Optiphot2-Pol), and controlled by a central processor (Mettler FP90). The image from the microscope was converted in video signal with a digital camera and controller (MTI CCD72). The video signal was passed through a For.A Video Timer, and broadcast to a computer, where the image was monitored with StreamPix digital video recorder software. Finally, to obtain the average droplet size of the polymer-poor phase, image analysis software was used.

For optical microscope analysis a small amount of the polymer–diluent solid solution with 20 wt.% in polymer (prepared as described above) was sandwiched between two glass cover slips separated by a 50 μm thick Teflon spacer.

3. Results and discussions

The molecular weight distribution for iPPZN was different from that of iPPM, as shown in Table 1. The thermal properties show that the iPPZN samples have significantly higher melting temperatures than the iPPM samples of the same $\bar{M}_w$. This difference has been attributed to the polypropylenes having different isotacticities [23].

3.1. Phase diagrams

The phase diagrams for iPPZN–DPE and iPPM–DPE systems of the same $\bar{M}_w$ are shown in Fig. 1(a), (c), and (e), respectively. They show a liquid–liquid region, a solid–liquid region, a dynamic crystallization curve, and a monotectic point (intersection between the liquid–liquid boundary and the dynamic crystallization curve) at approximately 40 wt.%. The diagrams show that the cloud point curves and the equilibrium crystallization curves are shifted only slightly to higher temperatures for the iPPZN–DPE systems.

The iPPZN and iPPM samples have pairs that match in terms of weight average molecular weights ($\bar{M}_w$). However, they differ in molecular weight distribution: the iPPM samples have narrow molecular weight distribution, approximately 2, compared to the iPPZN samples, which have distribution greater than 4. Thus, the samples differ in number average molecular weight ($\bar{M}_n$). Therefore, the shift of the cloud point curve can be attributed in part to an entropy contribution. Matsuyama et al. [13] and Lee et al. [15] also showed similar results when they used commercial iPP with different molecular weights, and attributed the difference to entropy effects.

To understand the shift of the cloud point curve in more detail, the interaction parameter χ was calculated based on the Flory–Huggins theory [34,35]. In this theory the interaction parameter is important for understanding the phase diagram, and it makes possible to know if the contributions are due to entropy or enthalpy.

McGuire [36] proposed a simple method for extrapolating the liquid–liquid phase boundary from experimental cloud point data. He shows two equations, (1) and (2), describing the polymer's chemical potential in the two separate phases (binodal line):

$$[(\phi_2^\beta)^2 - (\phi_2^\alpha)^2]\chi = \ln\left(\frac{1-\phi_2^\alpha}{1-\phi_2^\beta}\right) + \left(1-\frac{1}{r}\right)(\phi_2^\alpha - \phi_2^\beta) \quad (1)$$

$$r[(1-\phi_2^\beta)^2 - (1-\phi_2^\alpha)^2]\chi = \ln\left(\frac{\phi_2^\alpha}{\phi_2^\beta}\right) + (r-1)(\phi_2^\alpha - \phi_2^\beta) \quad (2)$$

where r is the ratio of the polymer's molar volume to the diluent molar volume, ϕ_2^α the polymer's volume fraction in the polymer-poor phase, and ϕ_2^β the polymer volume fraction in the polymer-rich phase.

Converting the experimental cloud point data from weight percent to volume fraction and then using these as ϕ_2^β and simultaneously solving Eqs. (1) and (2), the interaction parameters can be calculated. These parameters are shown against the reciprocal of temperature in Fig. 1(b), (d) and (f). In these plots, it is seen that the χ parameters are slightly shifted to higher values in the iPPZN–DPE than in the iPPM–DPE system. This would mean that there is also some enthalpy contribution, since if all the data were on one line, the shift would be only due to entropy contributions [13,37,38].

To verify this conclusion, the interaction parameters for the different systems are plotted in Fig. 2(a) and (b). All the data for each system (iPPZN and iPPM) fall approximately on one straight line. In this way the interaction parameter results show that when iPP of the same type (synthesized with either Ziegler–Natta or metallocene catalysts) are used, the shift is not observed.

Finally, to quantify the entropy and enthalpy contributions in some way, the interaction parameter can be assumed

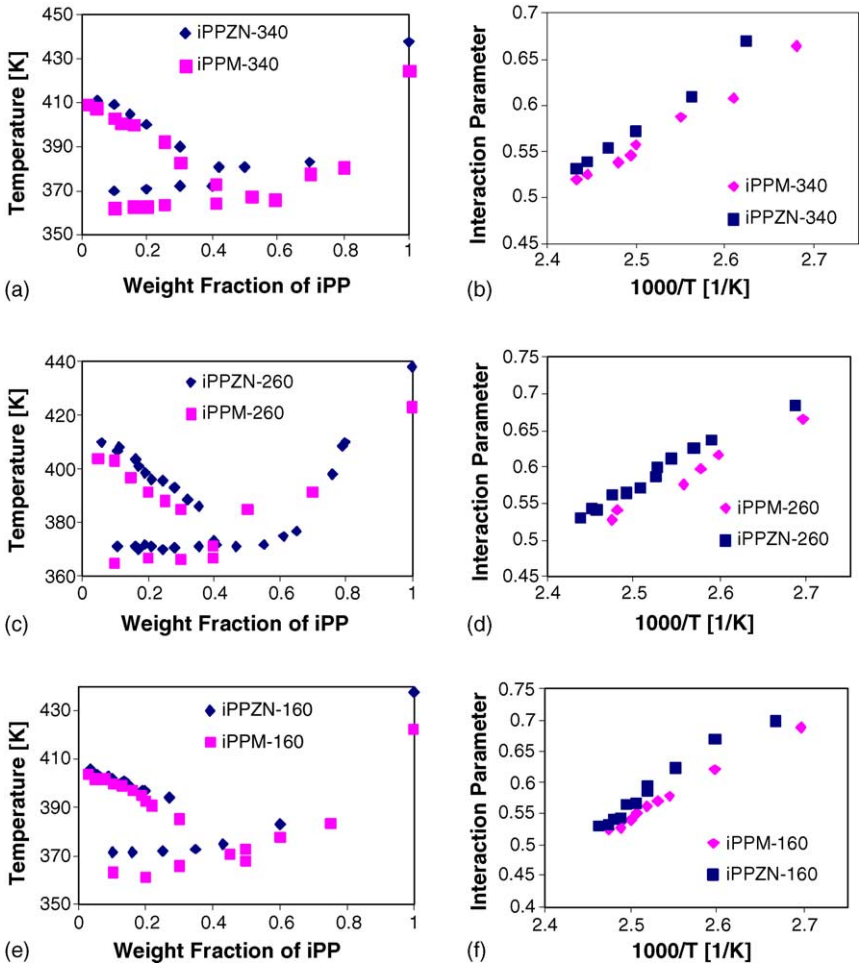

Fig. 1. (a), (c) and (e) Phase diagrams; (b), (d) and (f) interaction parameter χ for the iPP–DPE system (Ziegler–Natta and metallocene iPP).

to have a temperature dependence of the following form [32,36–39]:

$$\chi = a + \frac{b}{T} \tag{3}$$

where T is the absolute temperature, a represents an entropy contribution, and b represents an enthalpy contribution. The interaction parameters χ determined for each system from cloud point data using McGuire's method have been fitted to Eq. (3), and they can be written as Eqs. (4) and (5):

- iPPZN–DPE system

$$\chi = -1.26 + \frac{730}{T} \tag{4}$$

- iPPM–DPE system

$$\chi = -1.05 + \frac{630}{T} \tag{5}$$

Comparing a and b values in these equations indicates that the enthalpy contribution is more positive in the iPPZN–DPE

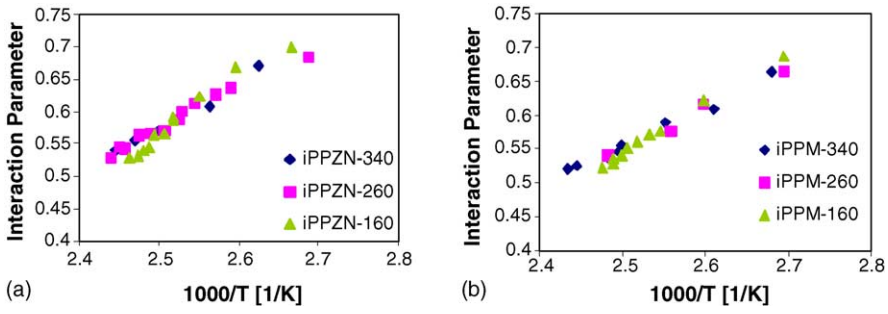

Fig. 2. Interaction parameter for: (a) iPPZN–DPE system, and (b) iPPM–DPE system.

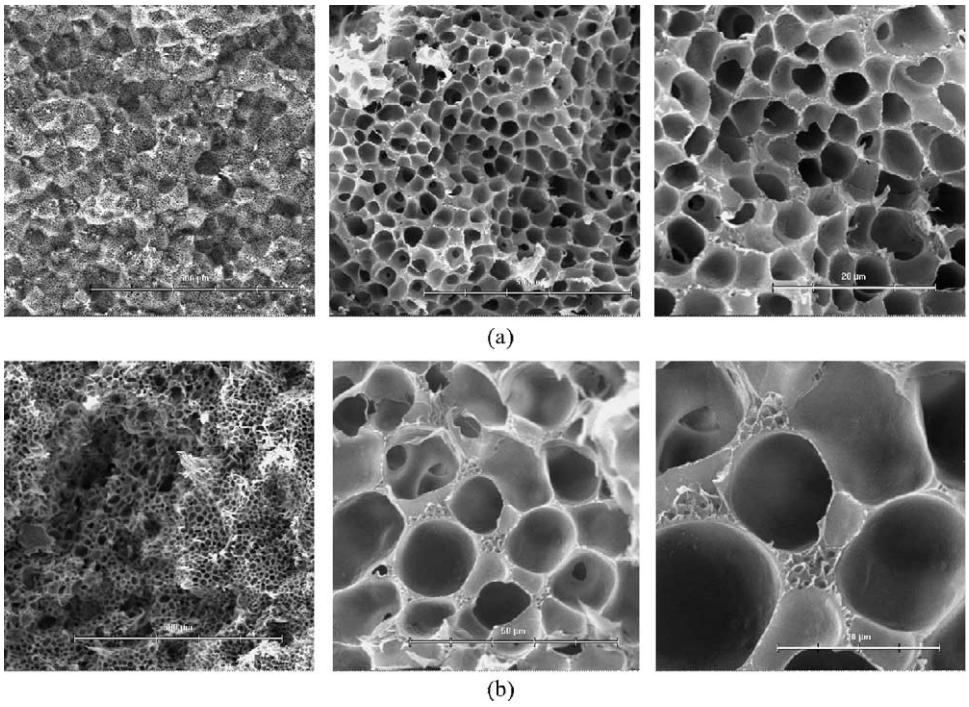

Fig. 3. Final morphology of the membranes prepared from 20 wt.% of polymer: (a) iPPZN-260; and (b) iPPM-260.

than in the iPPM–DPE system. This means that in the iPPZN–DPE system polymer–diluent interactions are less favored; therefore, the cloud point curve is shifted to higher temperatures [38,40–42]. However, it can be seen that there is a smaller entropy contribution in the iPPM–DPE system compared to the iPPZN–DPE system.

In this way, the slight shift of the cloud point curve attributed to the enthalpy contribution can be explained by the difference in the type of iPP used. This is due to the difference in stereoregularity and regioregularity between iPPZN and iPPM [30,31]. Bond et al. [23,43] showed that tacticity and polymorphism clearly affect the equilibrium melting temperature. On the other hand, it is well known that iPPZN generally crystallizes in the stable α-form, and iPPM crystallizes more easily in the γ-form [30]. So probably these differences in microstructure and polymorphism can affect the melt blending of iPP in DFE, since the effect of polymer intra-chain contacts on the interaction parameter is important in these systems [38,44].

3.2. Membrane morphology

Fig. 3 shows the resulting morphology of two membranes made using the procedure outlined above: one from iPPZN-260 and one from iPPM-260. The two polymers used here have the same $\bar{M}_w$, but different molecular weight distributions (the iPPZN being broader). Both membranes show spherical pores, indicating that the membranes were formed via liquid–liquid TIPS [13]; however, the iPPM sample has considerably larger pores than the iPPZN sample.

Two factors contribute to the final pore size: droplet growth rate and duration of the growth period. The growth rate depends on the viscosity of the system (the higher the viscosity, the slower the growth), while the growth period depends on the cooling rate and the temperature difference between the binodal and crystallization curve [16]. The cooling rate was essentially the same for the samples shown, but the difference between the binodal and crystallization curve is slightly greater for the iPPM–DPE system than for the iPPZN–DPE system. At 20 wt.% of polymer, the temperature difference in the iPPM–DPE system is 30 K, while the temperature difference in the iPPZN–DPE system is 25 K. This difference would allow the droplets a longer time to grow in the iPPM sample and produce larger pores.

Droplet growth rate is dependent on the matrix phase viscosity. A low viscosity in iPPM–DPE system could allow a faster droplet growth than the iPPZN–DPE system. The viscosity of the iPPZN was experimentally measured and determined to be approximately 1.3 times higher than iPPM; other authors report similar results [45,46], and thus larger pores could be produced in the iPPM sample for this effect. Therefore, both longer growth period and lower viscosity contribute to the iPPM sample having larger pores than the iPPZN sample.

3.3. Droplet growth process

To confirm the previous conclusion, droplet growth analysis for iPPZN–DPE and iPPM–DPE systems was carried out.

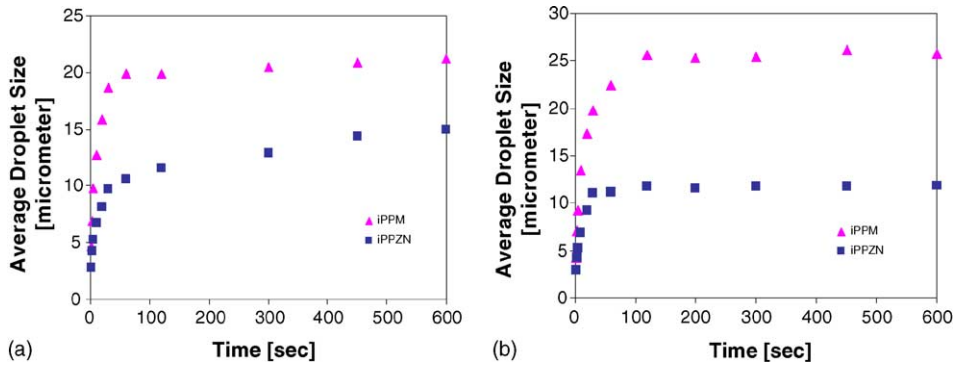

Fig. 4. Average droplet size for different iPP–DPE system for a polymer concentration of 20 wt.%, with cooling rate of 20 K/min: (a) cooled until 10 K lower than binodal curve, and (b) in non-isothermal condition until 293 K.

In this experiment, the sample on the hot stage was heated at 20 K/min from room temperature to 413 K, then, it was maintained for 5 min to remove the thermal history. In the first experiment, the sample was cooled at 20 K/min until 10 K lower than binodal curve. And in the second experiment, the sample (at 413 K) was cooled at 20 K/min to 293 K, in non-isothermal conditions. The time zero was defined as the time at which the phase separation starts.

Fig. 4 shows the time course of the average droplet size. These plots were obtained using the image analysis of the optical micrograph. In both cases, in isothermal and non-isothermal experiments, the droplet sizes in iPPM are larger than that in commercial iPPZN sample. These results can be directly related with the pores size in the membrane, and it can be attributed mainly to the two factors mentioned above: the growth period, and the difference in molecular weight distribution. The membrane pores are smaller than the observed droplet size. Kim et al. [47] and Matsuyama et al. [48] reported similar results, and they attributed the difference to shrinkage of the sample during diluent extraction and drying processes.

4. Conclusions

Polypropylene membranes were prepared by the TIPS process from iPP samples obtained via Ziegler–Natta and metallocene catalysts.

The phase diagrams indicated that the cloud point curves were shifted slightly to higher temperatures for the iPPZN–DPE than for the iPPM–DPE system. This shift has been attributed to entropy and enthalpy contributions. To understand the shift of the cloud point curves in more detail, the interaction parameter χ was calculated based on the Flory–Huggins theory, and it was found that the χ parameters were more positive in the iPPZN–DPE than in the iPPM–DPE system, so these results confirmed that the shift is also due to an enthalpy contribution. As an approximation, this enthalpy contribution was attributed to the difference in stereoregularity and regioregularity between iPPZN and iPPM, and to the differences in polymorphism of the isotactic polypropylenes.

The type of iPP clearly affects the final morphology of the membranes. Both membranes had a cellular structure, but the iPPZN membranes had smaller pores than the iPPM sample. The difference in pores size was confirmed whit a droplet growth analysis, it was found that the iPPM–DPE has a droplet growth rate faster than iPPZN–DPE systems, and thus the droplet sizes in iPPM are bigger than iPPZN.

This difference in droplet pore size was related to the shorter growth period and higher viscosity for the iPPZN system, but further research is needed to determine exactly how these factors influence the morphology in these particular systems.

Acknowledgements

The authors gratefully acknowledge the financial support to CONICYT through of the FONDAP-11980002 project. We also thank to the Deutscher Akademischer Austauschdienst (DAAD) for the Ph.D. scholarship to W. Yave. Finally we are indebted to Prof. J.L. Arias for your collaboration in SEM analysis.

References

[1] T.D. Jones, K.A. Chaffin, F.S. Bates, B.K. Annis, E.W. Hagaman, M.H. Kim, G.D. Wignall, W. Fan, R. Waymouth, Effect of tacticity on coil dimensions and thermodynamic properties of polypropylene, Macromolecules 35 (2002) 5061.

[2] Designer Plastics, The Economist Technology Quarterly, 8 December 2001, p. 27. http://www.economist.com/science/tq/displayStory.cfm?Story_id=885143.

[3] S.S. Rincón, Nuevos Desarrollos en PP: Copolímeros Heterofásicos de Alto Módulo, Revista de Plásticos Modernos 83 (2002) 307.

[4] H. Matsuyama, M. Yuasa, Y. Kitamura, M. Teramoto, D.R. Lloyd, Structure control of anisotropic and asymmetric polypropylene membrane prepared by thermally induced phase separation, J. Membrane Sci. 179 (2000) 91.

[5] P.M. Atkinson, D.R. Lloyd, Anisotropic flat sheet membrane formation via TIPS: atmospheric convection and polymer molecular weight effects, J. Membrane Sci. 175 (2000) 225.
[6] M.C. Yang, J.S. Perng, Microporous polypropylene tubular membranes via thermally induced phase separation a novel solvent-camphene, J. Membrane Sci. 187 (2001) 13.
[7] H. Mahmud, A. Kumar, R.M. Nrbaitz, T. Matsuura, Mass transport in the membrane air-striping process using microporous polypropylene hollow fibers: effect of toluene in aqueous feed, J. Membrane Sci. 209 (2002) 207.
[8] A.J. Castro, Methods for making microporous products, US Patent 4,247,498 (1981).
[9] W.C. Hiat, G.H. Vitzthum, K.B. Wagener, K. Gerlach, C. Josefiak, Microporous membrane via upper critical temperature phase separation, material science of synthetic membranes, in: ACS Symposium Series 269, American Chemical Society, Washington, DC, 1985, p. 229.
[10] D.R. Lloyd, S.S. Kim, K.E. Kinzer, Microporous membrane formation via thermally induced phases separation. II. Liquid–liquid phase separation, J. Membrane Sci. 64 (1991) 1.
[11] S.S. Kim, D.R. Lloyd, Microporous membrane formation via thermally induced phases separation. III. Effect of thermodynamic interaction on the structure of isotactic polypropylene membranes, J. Membrane Sci. 64 (1991) 13.
[12] A. Laxminarayan, K.S. McGuire, S.S. Kim, D.R. Lloyd, Effect of initial composition, phase separation temperature, and polymer crystallization on the formation of microcellular structures via thermally induced phase separation, Polymer 35 (1994) 3060.
[13] H. Matsuyama, T. Maki, M. Teramoto, K. Asano, Effect of polypropylene molecular weight on porous membrane formation by thermally induced phase separation, J. Membrane Sci. 204 (2002) 323.
[14] H. Matsuyama, S. Kudary, H. Kiyofuji, Y. Kitamura, Kinetic studies of thermally induced phase separation in polymer–diluent system, J. Appl. Polym. Sci. 76 (2000) 1028.
[15] H.K. Lee, A.S. Myerson, K. Levon, Nonequilibrium liquid–liquid phase separation in crystallizable polymer solution, Macromolecules 25 (1992) 4002.
[16] K.S. McGuire, A. Laxminarayan, D.S. Martula, D.R. Lloyd, Kinetic of droplet growth in liquid–liquid phase separation of polymer–diluent systems: model development, J. Colloid Interface Sci. 182 (1996) 46.
[17] W. Kaminski, H. Hähnsen, K. Külper, R. Woldt, Process for the preparation of polyolefins, US Patent 4,542,199 (1985).
[18] S.A. Miller, J.E. Bercaw, Isotactic-hemiisotactic polypropylene from C_1-symmetric ansa-metallocene catalysts: a new strategy for the synthesis of elastomeric polypropylene, Organometallics 21 (2002) 934.
[19] A. Eckstein, J. Suhm, C. Friedrich, R.D. Maier, J. Sassmannshausen, M. Bochmann, R. Mülhaupt, Determination of plateau moduli and entanglement molecular weights of isotactic, syndiotactic and atactic polypropylenes synthesized with metallocene catalysts, Macromolecules 31 (1998) 1335.
[20] R. Benavente, E. Pérez, R. Quijada, Effect of the comonomer content on the mechanical parameters and microhardness values in poly(ethylene-co-1-octadecene) synthesized by a metallocene catalyst, J. Polym. Sci., Part B: Polym. Phys. 39 (2001) 277.
[21] M. Yazdani-Pedram, R. Quijada, M.A. López-Manchado, Use of monomethyl itaconate grafted polypropylene (PP) and ethylene propylene rubber (EPR) as compatibilizers for PP/EPR blends, Macromol. Mater. Eng. 288 (2003) 875.
[22] M.F. Laguna, M.L. Cerrada, R. Benavente, E. Pérez, R. Quijada, Permeation measurement in ethylene-1-hexene, ethylene-1-octene, and ethylene-1-dodecene copolymers synthesized with metallocene catalysts, J. Polym. Sci., Part B: Polym. Phys. 41 (2003) 2174.
[23] E.B. Bond, J.E. Spruiell, J.S. Lin, A WAXD/SAXS/DSC study on the melting behavior of Ziegler–Natta and metallocene catalysed isotactic polypropylene, J. Polym. Sci., Part B: Polym. Phys. 37 (1999) 3050.
[24] R. Mülhaupt, Catalytic polymerization and post polymerization catalysis fifty years after the discovery of Ziegler's catalysts, Macromol. Chem. Phys. 204 (2003) 289.
[25] G.M. Benedikt, B.L. Goodall, Metallocene-catalyzed Polymers, Society of Plastics Engineers, Norwich, NY, USA, 1998.
[26] R. Quijada, J.L. Guevara, M. Yazdani-Pedram, G.B. Galland, D. Ribeiro, Study of the polymerization of 1-oactadecene with different metallocene catalysts, Polym. Bull. 49 (2002) 273.
[27] P.A. Saavedra, Tesis de Grado, Universidad de Chile, Julio, 2003.
[28] J. Voegele, C. Troll, B. Rieger, Zirconocene-catalyzed propene–ethene copolymer elastomers: kinetic investigation at low ethene concentration and characterization of microstructure, Macromol. Chem. Phys. 213 (2002) 1918.
[29] E. Bryan Bond, J.E. Spruiell, Melt spinning of metallocene catalyzed polypropylenes. I. On-line measurement and their interpretation, J. Appl. Polym. Sci. 82 (2001) 3223.
[30] F. Auriemma, C. De Rosa, Crystallization of metallocene-made isotactic polypropylene disordered modifications intermediate between the α and γ forms, Macromolecules 35 (2002) 9057.
[31] I.L. Hosier, R.G. Alamo, P. Esteso, J.R. Isasi, L. Mandelkern, Formation of the α and γ polymorphs in random metallocene–propylene copolymers. Effect of concentration and type of comonomer, Macromolecules 36 (2003) 5623.
[32] B. Lui, Q. Du, Y. Yang, The phase diagrams of mixtures of EVAL and PEG in relation to membrane formation, J. Membrane Sci. 180 (2000) 81.
[33] W. Yave, R. Quijada, Polipropilenos Hechos a Medida para su Utilización en Membranas, II Simposio Binacional Argentino-Chileno de Polímeros, Viña del Mar, Chile, Noviembre 2003.
[34] K.S. McGuire, A. Laxminarayan, D.R. Lloyd, A simple method of extrapolating the coexistence curve and predicting the melting point depression curve from cloud point data for polymer–diluent systems, Polymer 35 (1994) 4404.
[35] A.A. Lefebvre, N.P. Balsara, J.H. Lee, C. Vaidyanathan, Determination of the phase boundary of high molecular weight polymer blends, Macromolecules 35 (2002) 7758.
[36] K.S. McGuire, Dissertation, The University of Texas at Austin, May 1995.
[37] A. Zirkel, S.M. Gruner, Small-angle neutron scattering investigation of the Q-dependence of the Flory–Huggins interaction parameters in a binary polymer blend, Macromolecules 35 (2002) 7375.
[38] C. Etxabarren, M. Iriarte, C. Uriarte, A. Etxaberría, J.J. Iruin, Polymer–solvent interaction parameters in polymer solutions ant high polymer concentration, J. Chromatogr. A 969 (2002) 245.
[39] M. Seki, H. Uchida, Y. Maeda, S. Yamauchi, K. Takagi, Y. Ukai, Y. Matsushita, Study on the thermodynamic interaction between isotactic polypropylene and ethylene-1-hexene random copolymers by SANS, Macromolecules 33 (2000) 9712.
[40] D.R. Lloyd, Microporous membrane formation via thermally induced phase separation. I. Solid–liquid phase separation, J. Membrane Sci. 52 (1990) 239.
[41] H.C. Vadalia, H.K. Lee, A.S. Myerson, K. Levon, Thermally induced phase separation in ternary crystallizable polymer solutions, J. Membrane Sci. 89 (1994) 37.
[42] N. Schuld, B.A. Wolf, Solvent quality as reflected in concentration and temperature dependent Flory–Huggins interaction parameter, J. Polym. Sci., Part B: Polym. Phys. 39 (2001) 651.
[43] E.B. Bond, J.E. Spruiell, The effects of atacticity, comonomer content and configurational defects on the equilibrium melting temperature of monoclinic isotactic polypropylene, J. Appl. Polym. Sci. 81 (2001) 229.

[44] P.C. Painter, L.P. Berg, B. Veytsman, M.M. Coleman, Intermolecular screening in nondilute polymer solutions, Macromolecules 30 (1997) 7529.
[45] E.B. Bond, J.E. Spruiell, Melt spinning of metallocene catalyzed polypropylenes. II. As-spun filament structure and properties, J. Appl. Polym. Sci. 82 (2001) 3237.
[46] M. Gahleitner, Melt rheology of polyolefins, Prog. Polym. Sci. 26 (2001) 895.
[47] S.S. Kim, M.O. Yeom, I.S. Cho, in: I. Pinnau, B.D. Freeman (Eds.), ACS Symposium Series 744, American Chemical Society, Washington, DC, 1999.
[48] H. Matsuyama, M. Teramoto, S. Kudari, Y. Kitamura, Effect of diluents on membrane formation via thermally induced phase separation, J. Appl. Polym. Sci. 82 (2001) 169.